ACS APPLIED MATERIALS & INTERFACES

Research Article

www.acsami.org

Detection of Aniline Oligomers on Polyaniline–Gold Interface using Resonance Raman Scattering

Miroslava Trchová,* Zuzana Morávková, Jiří Dybal, and Jaroslav Stejskal

Institute of Macromolecular Chemistry, Academy of Sciences of the Czech Republic, 162 06 Prague 6, Czech Republic

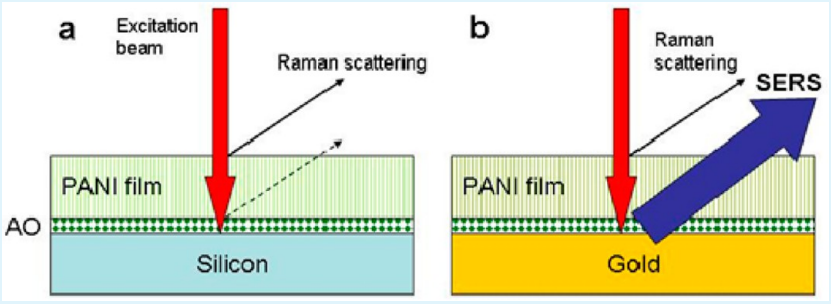

ABSTRACT: In situ deposited conducting polyaniline films prepared by the oxidation of aniline with ammonium peroxydisulfate in aqueous media of various acidities on gold and silicon supports were characterized by Raman spectroscopy. Enhanced Raman bands were found in the spectra of polyaniline films produced in the solutions of weak acids or in water on gold surface. These bands were weak for the films prepared in solutions of a strong acid on a gold support. The same bands are present in the Raman spectra of the reaction intermediates deposited during aniline oxidation in water or aqueous solutions of weak or strong acids on silicon removed from the reaction mixture at the beginning of the reaction. Such films are formed by aniline oligomers adsorbed on the surface. They were detected on the polyaniline–gold interface using resonance Raman scattering on the final films deposited on gold. The surface resonance Raman spectroscopy of the monolayer of oligomers found in the bulk polyaniline film makes this method advantageous in surface science, with many applications in electrochemistry, catalysis, and biophysical, polymer, or analytical chemistry.

KEYWORDS: *polyaniline, aniline oligomers, Raman spectroscopy, SERS*

1. INTRODUCTION

Polyaniline (PANI) ranks among the most important conducting polymers. It is synthesized by the oxidation of aniline with various oxidants, ammonium peroxydisulfate (APS) being the most common choice. Because of its electrical, electrochemical, and optical properties, PANI has a good potential for application in antistatic coatings,[1] biosensors,[2,3] corrosion protection,[3−6] electrochemical capacitors and supercapacitors,[7−11] electrochromic devices and electrodes in solar cells,[12−14] fuel cells,[15] light-emitting diodes,[16] separation membranes,[17,18] nonlinear optical devices,[19] sensors,[20,21] shielding of electromagnetic interference,[22,23] and so forth. Most of the recent trends have aimed at the use of conducting polymers in biosciences. Conducting polymers have proved to be effective reducing agents in the synthesis of noble-metal nanoparticles.[24] The fabrication of gold or silver structures on a PANI membrane for surface-enhanced Raman spectroscopy (SERS) has been demonstrated in recent years.[25−29] A new pathway for the preparation of SERS-active nanoparticle films from colloids has been recently proposed.[30]

Many applications of this polymer require thin conducting films. They can be produced on substrates immersed in the reaction mixture used for the polymerization of aniline. PANI films have typically been prepared in strongly acidic aqueous media.[31] The globular morphology of PANI powders produced under such conditions is then projected into the similar globular structure of films. Nanotubes are the product when the oxidation of aniline takes place under mildly acidic conditions, and oligomeric microspheres are obtained in alkaline media.[32] In such cases, the films produced on immersed surfaces usually mimic the morphology of the powders produced at the same time in the bulk of the medium. One of the techniques available to monitor the course of polymerization is based on the isolation of reaction intermediates followed by their ex situ characterization. The evolution of aniline oligomers produced in the early part of aniline oxidation in weak acid solutions as well as a polymer with nanotubular structure formed in the subsequent regime was studied earlier.[33,34]

Surface-enhanced Raman spectroscopy (SERS) is a suitable method for the observation of details of molecular structure in thin polymer films.[35−41] An increased formation of PANI on nanostructures after X-ray irradiation has been recently investigated by SERS.[37] The presence of the interface, represented typically by noble metals that interact with the polymer film, is expected to induce a specific response in the SERS spectra. The interaction of emeraldine PANI base with

Received: October 3, 2013
Accepted: December 30, 2013
Published: December 30, 2013

 © 2013 American Chemical Society

silver and gold colloids was studied by SERS at various excitation wavelenghts.[38] It was shown that the polymer produced after the adsorption of PANI base on metal nanoparticles is considerably dependent on the nature of the metal colloids. Although the oxidation of PANI base to pernigraniline takes place in silver colloids, the doping occurs when gold nanoparticles are present.[39] The authors observed a doublet at 1328 and 1375 cm^{-1} in the SERS spectra with 1064 nm laser excitation, which is related to the vibrations of the cation radicals (semiquinone segments) present in the emeraldine salt.[39] The structures of the emeraldine salt and emeraldine base forms in PANI films deposited on rough silver and gold supports have been reported.[40,41] It was demonstrated that the SERS spectra of emeraldine base deposited on gold are characterized by a semiquinonoid structure. In solutions of sulfuric acid, the SERS spectra changed gradually as the protonation degree increased. The SERS spectra demonstrate that the emeraldine salt can be only partially deprotonated with water or ammonium hydroxide at the gold support. The SERS spectra of fully protonated PANI are characterized by a doublet with local maxima at about 1330 and 1370 cm^{-1}.[41] The properties of metallic supports have a marked influence on the SERS spectra of adsorbed species.

We have earlier observed two peaks at 1339 and 1379 cm^{-1} in the Raman spectra of the PANI base with nanotubular morphology deposited on a silicon support.[42] In the Raman spectra of freshly prepared films of the deprotonated globular PANI on gold support, we have observed bands at 1635, 1567, 1415, and 1335 cm^{-1}, with a shoulder at 1373 cm^{-1}; the films exhibited enhanced resistance toward deprotonation and ageing.[43] These peaks were assigned to the cross-linked phenazine-like structures.[44−46] They were also observed in the Raman spectra of the first products of aniline oxidation in water.[34] We have recently observed that Raman spectra of the products of aniline oxidation under alkaline conditions grown on smooth gold and on silicon only slightly differ from each other.[47] In particular, the intensity of some peaks was relatively higher for the gold support. Under alkaline conditions, only oligomers are produced. The idea that chemisorbed aniline oligomers interact with the surface, which leads to the resonance Raman scattering and to the enhanced intensity of the scattered light, has been formulated. In present article, this hypothesis has been tested and proved for the films deposited in situ on a gold support in the presence of strong and weak acids and in water when a PANI film is produced. The role of the oligomers in guiding the shape of the PANI nanostructures in the surface science and in many applications is presented. The interpretation of the band at 1373 cm^{-1}, which has been observed by many research groups in the Raman spectra of PANI, is reconsidered.

2. MATERIALS AND METHODS

2.1. Preparation. The films on silicon or gold-coated glass were prepared by the oxidation of 0.2 M aniline with 0.25 M ammonium peroxydisulfate (APS) in the presence of 0.1 M sulfuric acid, 0.4 M succinic acid, or water. The detailed experimental description is provided in ref 47. The windows removed at the early stages of oxidation (4−8 min) are referred to as starting films. Other windows left in the reaction mixture until the aniline oxidation was completed are referred to as final films. The end of the polymerization was determined from the earlier obtained course of the reaction.[32,33,48] After the Raman spectra were recorded, the films were converted to corresponding bases and dried. The Raman spectra of the deprotonated samples were recorded as well.

2.2. Raman Spectroscopy. A Renishaw inVia Reflex Raman spectrometer was used for the collection of the Raman spectra excited with a HeNe 633 nm laser. A Leica DM LM microscope with 50× Olympus objective was used for optical microscopy and to focus the laser beam on the sample stage. A holographic grating (1800 lines mm^{-1}) was used to analyze the scattered light. A Peltier-cooled CCD detector (578 × 385 pixels) registered the dispersed light.

2.3. Calculations. Vibrational spectra were calculated by quantum chemical methods at the density functional theory (DFT) level employing the Gaussian 09 program package.[49] The geometrical structures of model molecules were fully optimized without any constrains. Vibrational frequencies of the normal modes were calculated at the B3LYP/6-31+G(d) level, and the reported values were scaled by the standard scaling factor of 0.9636.[50]

3. RESULTS AND DISUSSION

Thin PANI films were deposited on immersed solid substrates during chemical oxidation of aniline, which is a typical approach for PANI preparation (Figure 1). The main polymerization of

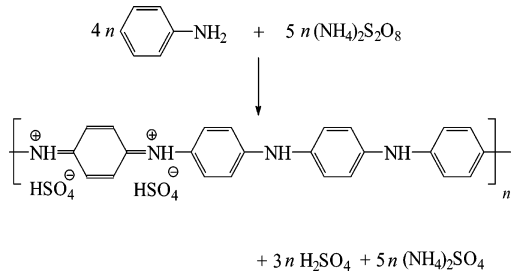

Figure 1. Oxidation of aniline with ammonium peroxydisulfate in an acidic medium yields the emeraldine form of PANI. Sulfuric acid and ammonium sulfate are byproducts.

aniline takes place in the bulk of the reaction mixture. However, all solid surfaces, which are in contact with the aqueous reaction mixture used for the preparation of PANI, are coated with such a film. Aniline oligomers play a fundamental role in the film formation.[31,51] They are produced at early stages of aniline oxidation and adsorb at available surfaces at first. Subsequently, these oligomers act as initiation centers, starting the growth of PANI chains. Polyaniline films having a thickness of ∼100 nm are produced in this way.[31,48] The formation of PANI films at the surfaces starts before the polymerization of aniline in the surrounding liquid phase.[31,51] Considering this model, the bottom side of the films located at the interface with the support is composed preferentially of aniline oligomers, whereas the external surface of the film by PANI.[52]

Polymerization in the solution of 0.1 M sulfuric acid produced a globular morphology of PANI. The oxidation in 0.4 M succinic acid or in water leads to nanotubes along with a globular precipitate.[32] The morphology of the final films deposited on gold and silicon windows was observed by optical microscopy (Figures 2 and 3, respectively). The colors of the films produced by reflected light on silicon or gold supports differ from the colors displayed by the films deposited on glass in transmission mode. The film morphology remained unchanged after deprotonation with 0.1 M ammonium hydroxide, but their colors changed as the PANI salt converts to PANI base.

3.1. Raman Spectra of the Final Films on Silicon. The Raman spectrum of the final film prepared in the sulfuric acid solutions and obtained with the 633 nm laser excitation line has been described earlier (Figure 4a).[42,47] The Raman spectra of

dx.doi.org/10.1021/am404252f | ACS Appl. Mater. Interfaces 2014, 6, 942−950

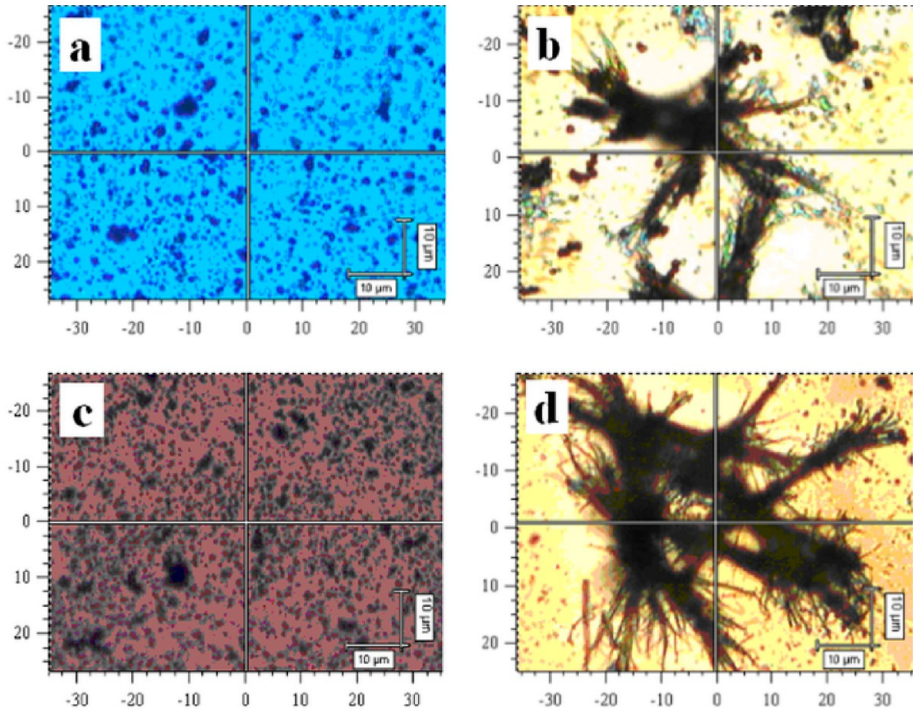

Figure 2. Optical images of the final films obtained by the oxidation of aniline with ammonium peroxydisulfate in 0.1 M sulfuric (a) and 0.4 M succinic (b) acids on silicon windows and of the corresponding films after their deprotonation with 0.1 M ammonium hydroxide (c, d). The scale bars correspond to 10 μm.

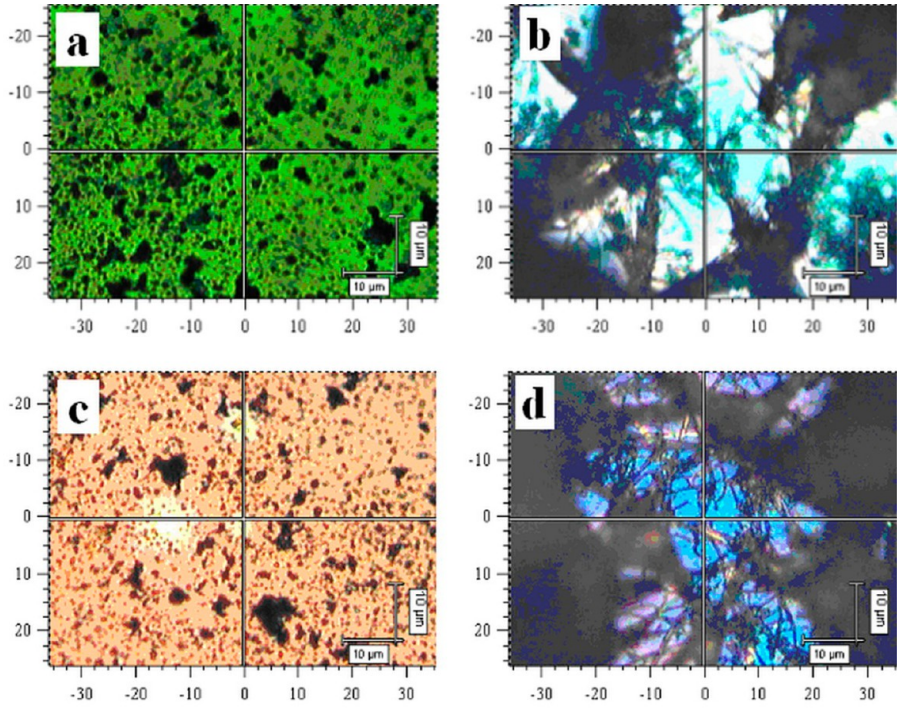

Figure 3. Optical images of the final films obtained by the oxidation of aniline with ammonium peroxydisulfate in 0.1 M sulfuric (a), and 0.4 M succinic (b) acids on gold supports and of the corresponding films after their deprotonation with 0.1 M ammonium hydroxide (c, d). The scale bars correspond to 10 μm.

the final films prepared in the solutions of succinic acid or in water reflect some differences in the molecular structure that are associated with nanotubular morphology (Figure 4a).[34,42,43] They suggest the presence of phenazine-like or cross-linked constitutional units in their structure (Figure 4a).[45,46,53,54] The Raman bands of the final films and their assignments are summarized in the Table 1.

The spectra of the alkali-treated final films (i.e., of PANI bases) deposited on a silicon support (Figure 4b) display substantial changes compared with the spectra of PANI salts. The close similarity in the shape for samples prepared under

dx.doi.org/10.1021/am404252f | ACS Appl. Mater. Interfaces 2014, 6, 942−950

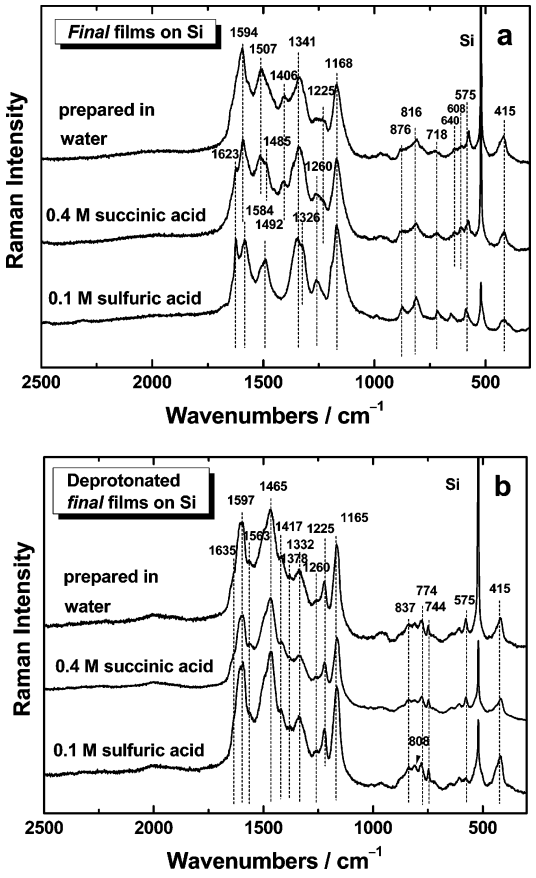

Figure 4. Raman spectra of the final films produced during in situ oxidation of aniline in 0.1 M sulfuric acid,[42] 0.4 M succinic acid, and water[42] on silicon supports (a) and after deprotonation with 0.1 M ammonium hydroxide (b) at an excitation wavelength of 633 nm (adapted from ref 47).

Table 1. Assignment of Raman Bands (λ_{exc} = 633 nm) of the as-Produced Final Films Deposited on Silicon during Aniline Oxidation in the Solutions of Various Acids[a]

wavenumbers (cm^{-1})			
sulfuric acid	succinic acid	water	assignment
1630 sh	1630 sh	1630 sh	Phz, ν(C═O) of *p*-benzoquinone[47]
1623 s	1623 sh		$\nu(C{\sim}C)_B$[34,42,43]
1584 s	1594 s	1594 s	$\nu(C{=}C)_Q$[33,39,46]
1507 sh	1507 m	1507 m	δ(N−H) in (SQ)[34,42,43]
1492 s	1485 sh		$\nu(C{=}N)_Q$[34,42,43]
	1406 w	1406 w	Phz[34,45,46,53,54]
1341 s	1341 s	1341 s	$\nu(C{\sim}N^{\bullet+})$ of polarons with shorter conjugation lengths[34,45]
1326 sh			$\nu(C{\sim}N^{\bullet+})$ of more delocalized polaronic structures[34,42,43]
1260 m	1260 w		$\nu(C{-}N)_B$[34,42,43]
	1225 sh	1225 w	$\nu(C{-}N)_Q$[34,42,43]
1168 s	1168 w	1168 s	δ(C−H) in SQ[34,42,43]
876 w	876 w	876 w	C−N−C wagging (o.p.); B-ring deformation (i.p.) in polarons and bipolarons;[34,42,43]
816 w	816 w	816 w	B-ring deformation;[34,42,43]
718 w	718 w	718 w	amine deformation in bipolaronic form of emeraldine salt[34,42,43]
654 w			sulfate anion[34,42,43]
575 w	575 w	575 w	phenoxazine-type units[42,45,53]
520 m	520 s	520 s	ring deformation (o.p.) + silicon vibrations[34,42,43]
415 w	415 w	415 w	ring deformation (o.p.)[34,42,43]

[a]Abbreviations: s, strong; m, medium; w, weak; sh, shoulder; ν, stretching; δ, in-plane bending; B, benzenoid ring; Q, quinonoid ring; SQ, semiquinonoid ring; Phz, phenazine-like segment; ∼, a bond intermediate between a single and a double bond; o.p., out-of-plane; and i.p., in plane.

various conditions is connected with a strong resonance effect of the energy of the excitation wavelength (633 nm). The observed changes in the Raman spectra after deprotonation with 0.1 M ammonium hydroxide confirm the presence of imine nitrogens that are able to become protonated and that constitute the hydrogen bonds with other nitrogen sites. The strong hydrogen bonding leads to the cross-linked structure that is close to chemical cross-linking with the formation of pseudo-phenazine-like units.[55−58]

3.2. Raman Spectra of the Final Films on Gold. The Raman spectrum of the final film prepared in 0.1 M sulfuric acid on a gold support (Figure 5a) is close to the spectrum obtained on a silicon support (Figure 4a). On the contrary, the spectra of the final films prepared in 0.4 M succinic acid and in water (Figure 5a) differ dramatically from the spectra of the as-produced final films deposited on silicon windows (Figure 4a). Their intensity is enhanced, and one can observe a shoulder at 1622 cm^{-1}, sharp peaks at 1591, 1573, 1515, 1476, and 1412 cm^{-1}, a strong sharp peak at 1373 cm^{-1} with a shoulder at 1342 cm^{-1}, and peaks at 1250, 1156, and 608 cm^{-1} in the spectra of the final films on gold. Their shape is very close to the shape of the spectra of the intermediates deposited during the reaction of aniline with ammonium peroxydisulfate in water on a silicon window at the beginning of the reaction (Figure 6a).[34] We have observed the same Raman spectra not only in the case of the first products deposited on silicon windows in water[34] or in the presence of weak acid but also in the presence of a strong sulfuric acid (Figure 6a).[47,48] They will be discussed in the following paragraphs.

After deprotonation with 0.1 M ammonium hydroxide, the spectra of all final films on gold supports (Figure 5b) are close to the spectra of deprotonated samples deposited on silicon windows (Figure 4b), which correspond to the spectra of PANI base. This supports the fact that a film of PANI is really present on the sample prepared in water or in the presence of weak acid on gold supports that is not evident from the spectra before deprotonation. A small peak observed at 1373 cm^{-1} in the spectrum of the deprotonated film prepared in presence of succinic acid and in water can be distinguished in the spectra (Figure 5b) and will be discussed later.

3.3. Raman Spectra of the Starting Films on Silicon. The Raman spectra of the starting films produced during the reaction of aniline with APS in water or in aqueous solutions of weak and strong acid on the silicon windows at the beginning of the reaction are shown in Figure 6a. They have been recently described in ref 47. It can be seen that their shape is very close to the shape of the Raman spectra of the final films deposited on a gold support except that their intensity is lower and the positions of the main peaks are slightly shifted. We observed a shoulder at 1635 cm^{-1} of the peak at 1585 cm^{-1}, peaks at 1542, 1477, and 1413 cm^{-1}, a sharp peak at 1363 cm^{-1} with a shoulder at 1342 cm^{-1}, and peaks at 1270, 1235, 1157, and 608 cm^{-1} in the Raman spectra of the starting films on silicon window.

dx.doi.org/10.1021/am404252f | ACS Appl. Mater. Interfaces 2014, 6, 942−950

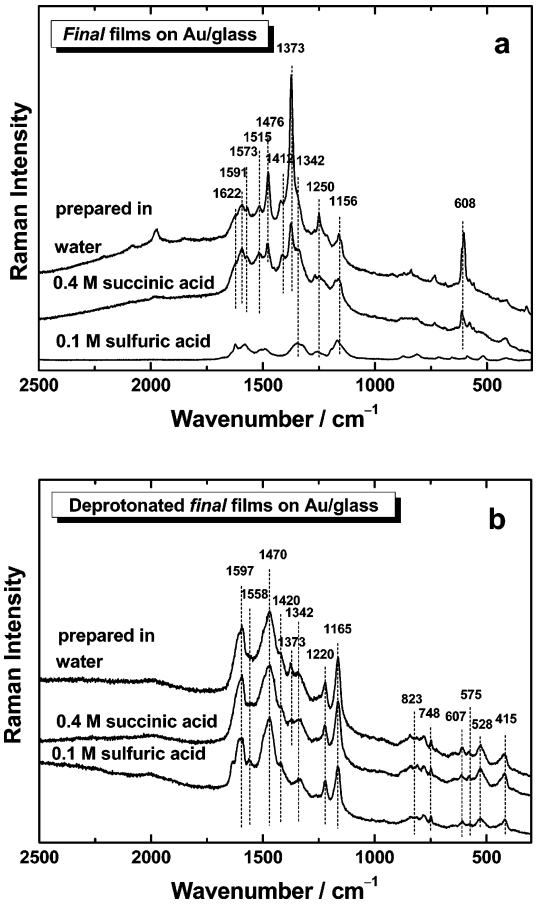

Figure 5. Raman spectra of the final films produced during in situ oxidation of aniline in 0.1 M sulfuric acid, 0.4 M succinic acid, or water on gold (a) and after deprotonation to bases with 0.1 M ammonium hydroxide (b) at an excitation wavelength of 633 nm.

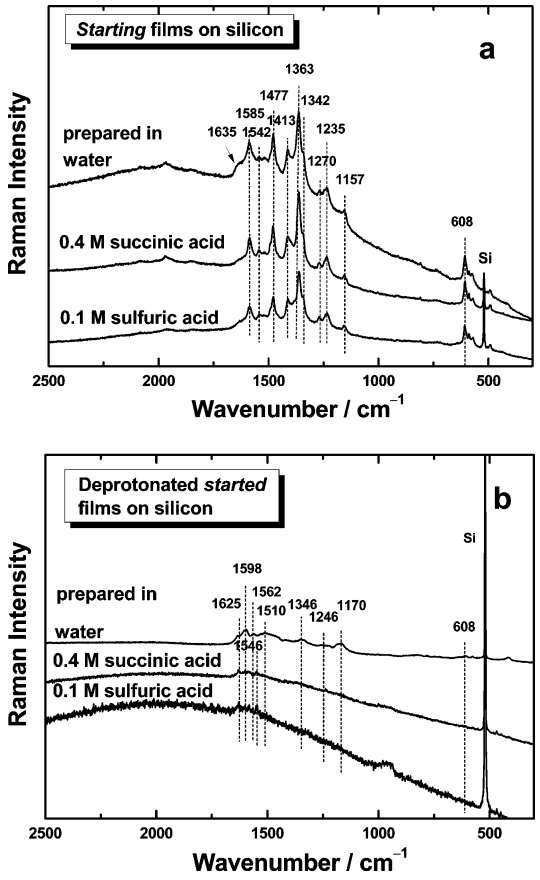

Figure 6. Raman spectra of the starting films produced during in situ oxidation of aniline in 0.1 M sulfuric acid,[48] 0.4 M succinic acid,[48] or in water[34] on silicon (a) and after deprotonation to bases with 0.1 M ammonium hydroxide (b) at an excitation wavelength of 633 nm (adapted from ref 47).

After deprotonation with 0.1 M ammonium hydroxide, the spectra of all starting films produced on a silicon window dramatically changed (Figure 6b). They exhibit a strong fluorescence with some weak Raman peaks. One can distinguish a shoulder at about 1625 cm^{-1}, and weak peaks at 1598, 1562, 1510, 1346, 1246, 1170, and 608 cm^{-1} in the spectrum of samples prepared in water.

The most exciting result is the general similarity between the spectra of the final films obtained in a weak acid solution or water on a gold support (Figure 5a) and the spectra of the starting films obtained in strong and weak acid solutions or water on silicon (Figure 6a). We suppose that the Raman spectra of the final films on a gold support reflect the first products of aniline oxidation adsorbed on the surface because of their interaction with the gold support (Figure 7). After treating the film with ammonium hydroxide, the low-molecular oligomers adsorbed on the gold surface are deprotonated, and their Raman bands are no longer resonantly enhanced with 633 nm laser excitation. The Raman scattering of the PANI base dominates the spectrum. The small peak observed at 1373 cm^{-1} in the spectrum of the deprotonated film prepared in presence of succinic acid and in water (Figure 5b) suggests that deprotonation is not complete.[33,34]

The fact that the Raman peaks corresponding to the oligomers deposited on the gold surface are not observed in the case of oxidation in the solutions of strong acid is connected with the balance between neutral and protonated aniline molecules in the reaction mixture.[48] Under less acidic conditions, neutral molecules dominate, and anilinium cations prevail at low pH. The oxidation of neutral aniline is easy, whereas analogous oxidation of anilinium cations is inhibited. When the oxidation of aniline is carried out under high acidity, oligomers are produced in only a negligible amount.[32,48] The polymer is thus the exclusive product, with oligomers being found only as traces that are not detected in the Raman spectrum in the presence of the bulk PANI film. In the case of the first products on the silicon support, the reaction was stopped before the film could grow on the first layer of oligomers. Increased solubility of aniline oligomers after the protonation under strongly acidic conditions is probably also responsible for their low concentration in the films.

During the oxidation of aniline, phenazine-like units were formed (Figure 8a,b).[33,48] They can be either in the base form (Figure 8b) or, after reaction with an acid, the protonotation of imine nitrogen outside the phenazine heterocycle takes place. This is followed by electron rearrangement, and the phenazinium cation is produced (Figure 8a). The molecules comprising aniline and *p*-benzoquinone moieties (Figure 8c,d) are most likely produced at the same time. On the basis of the similarities in the infrared spectra of the products of aniline oxidation with APS and with *p*-benzoquinone, Surwade et al. proposed the mechanism for the chemical oxidation of aniline with APS in aqueous pH 2.5−5 buffers.[59] They reported that the products are composed of adducts of aniline and *p*-

dx.doi.org/10.1021/am404252f | ACS Appl. Mater. Interfaces 2014, 6, 942−950

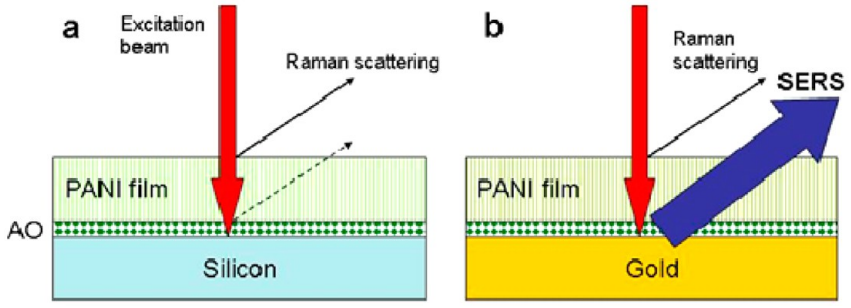

Figure 7. During in situ deposition, aniline oligomers (AO) are adsorbed at the support. PANI films subsequently grow on top of them. On silicon, the intensity of Raman scattering is strongest at the film surface, and the contribution of oligomers is small (a) because of the absorption of the primary beam and scattered light. On gold, the surface-enhanced Raman scattering from aniline oligomers occurs at the interface between the film and the gold support (b) and dominates the spectrum.

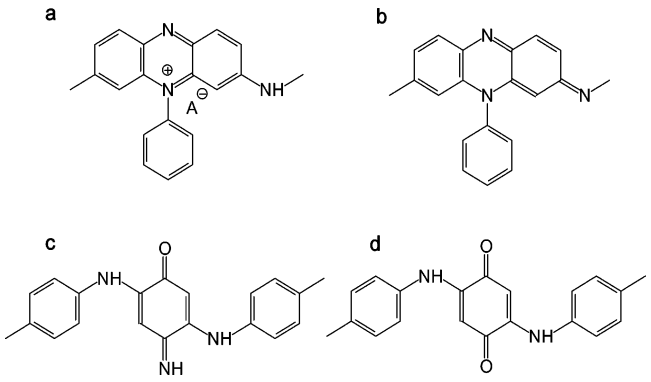

Figure 8. Examples of hypothetical constitutional units derived from three original aniline molecules: (a) N-substituted phenazinium cation, (b) N-substituted phenazine, (c) *p*-quinoneimine, and (d) *p*-benzoquinone. They may be present as isolated molecules or constitute a part of larger oligomers.

benzoquinone monoimine (Figure 8c) or *p*-benzoquinone (Figure 8d) at various degrees of hydrolysis and oxidation. Ferreira et al. have recently reached a similar conclusion.[60] On the basis of the discussion on the molecular structure of aniline oligomers,[61] we assume the presence of constitutional units, such as phenazinium (Figure 8a) or phenazine-like (Figure 8b), and the units with oxygen-containing groups, such as quinoneimines (Figure 8c) or quinones (Figure 8d). The sulfatization of benzene rings induced by peroxydisulfate[59,62,63] may further chemically modify these units. We suppose that the Raman spectra of starting films contain the peaks corresponding to the vibrations of the constitutional units shown in Figure 8 in addition to the vibrations of sulfate groups.

3.4. Interpretation of the Raman Spectra of the Final Films on Gold. For the explanation of the Raman spectra of the final films on a gold support (Figure 5a), the interpretation of the Raman spectra of the starting films on a silicon window (Figure 6a) and their molecular structure play crucial roles. They should correspond to the presence of the constitutional units and chromophores that are proposed in Figure 8. The interpretation of the Raman spectra is still in progress.[34,47,60,64,65] According to several research groups, the sharp band at 1363 cm^{-1} with a shoulder at 1342 cm^{-1} indicates the presence of semi-quinone cation radical structures in polymer chains.[34,39,66,67] The band at ~1370 cm^{-1} was assigned to the $\nu(C{\sim}N^+)$ vibrations of more localized polaronic sites.[34,66] On the basis of computer-simulation studies of the mechanism of aniline oxidation in water[68,69] and on nonconductivity of oligomeric products, we assigned the band at ~1370 cm^{-1} to the $C{\sim}N^+$ vibrations of charged phenazine-like units in the *N*-phenyl-substituted phenazinium cation (Figure 8a).[34,70] The Raman bands of the starting films and their assignments are summarized in Table 2.

3.5. Calculated Raman Spectra of Hypothetical Chromophores. The Raman spectra were calculated for all

Table 2. Assignment of Raman Bands (λ_{exc} = 633 nm) of the as-Produced Starting Films Deposited on Silicon during Aniline Oxidation under Various Acidity Conditions[a]

wavenumbers (cm^{-1})			
sulfuric acid	succinic acid	water	assignment
1635 sh	1635	1635 sh	$\nu(C{=}O)$ of *p*-benzoquinone;[64,65] Phz[34]
1585 m	1585 m	1585 m	$\nu(C{\sim}C)_{SQ}$;[34] $\nu(C{=}C)_Q$[34,42,43]
1542 w	1542 w	1542 w	$\nu(C{-}C)_Q$;[34,42,43] Phz[34]
1514 w	1514 w	1514 w	$\delta(N{-}H)$[34]
1477 m	1477 m	1477 m	$\nu(C{=}N)_Q$;[34,42,43] $\nu(C{=}N)_Q$ of *p*-benzoquinone;[60] Phz[34]
1413 m	1413 m	1413 m	Phz[34,42]
1359 s	1363 s	1363 s	$\nu(C{\sim}N^+)$ of substituted *N*-phenylphenazines[34,47,70]
1270 w	1270 w	1272 w	$\nu(C{-}N)$ of Phz;[34,60] $\nu(C{-}N)_B$;[34,42,43] $\nu(C{-}C)$ of *p*-benzoquinone[60,65]
1235 w	1235 w	1235 w	$\nu(C{-}N)_Q$;[34,42,43] $\nu(C{-}N)_B$[34]
1157 w	1157 w	1157 w	$\delta(C{-}H)_Q$[34]
608 w	608 w	608 w	$\nu(C{-}S)$; $\delta(SO_2)$; Phz cation;[45,60] B-ring deformation (i.p.)[34]

[a]Abbreviations: s, strong; m, medium; w, weak; sh, shoulder; ν, stretching; δ, in-plane bending; B, benzenoid ring; Q, quinonoid ring; SQ, semiquinonoid ring; Phz, phenazine-like segment; ~, a bond intermediate between a single and a double bond; o.p., out-of-plane; and i.p., in plane.

dx.doi.org/10.1021/am404252f | ACS Appl. Mater. Interfaces 2014, 6, 942−950

of the hypothetical chromophores presented in Figure 8. In the quantum chemical calculations, the constitutional units were replaced by corresponding finite model molecules. For that purpose, the terminal bonds in the polymer segments were substituted with hydrogen atoms. A strong band located at 1387 cm^{-1} appears in the calculated Raman spectrum of the molecule corresponding to the *N*-substituted phenazinium cation (Figure 9a). This band is assigned to the normal

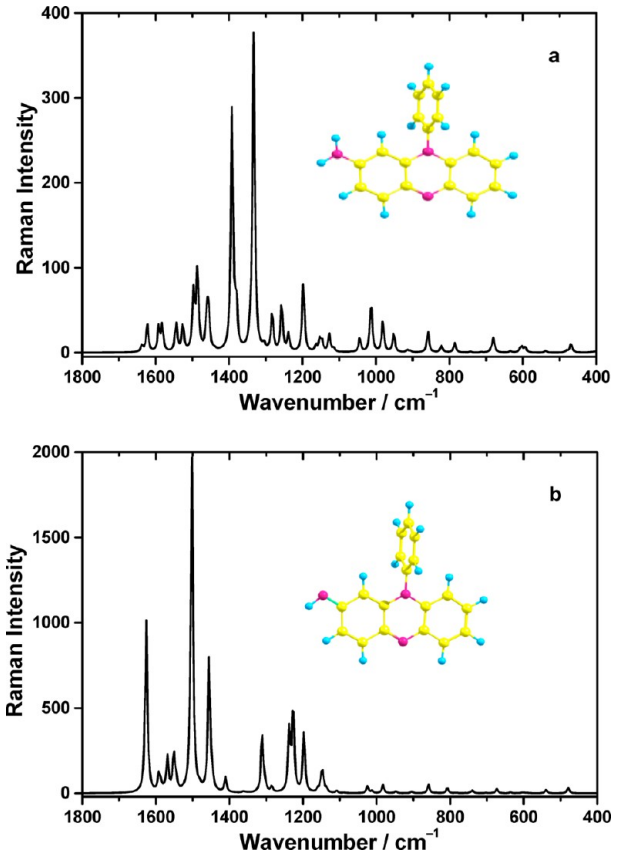

Figure 9. Calculated Raman spectra of the model molecule corresponding to the *N*-substituted phenazinium cation (a) and *N*-substituted phenazine (b).

vibrational mode dominated by stretching of the C−N^+ and C−C bonds. In the Raman spectrum of the analogous deprotonated form (a molecule corresponding to *N*-substituted phenazine), no band appears in this region (Figure 9b). This result supports the idea that the emergence of a corresponding strong band in the Raman spectra is connected with the presence of the protonated phenazine-like structures. An analogous band is also observed in the calculated Raman spectra of the model molecules corresponding to *p*-quinoneimine (1353 cm^{-1}) and *p*-benzoquinone (1361 cm^{-1}). The intensity of latter bands, however, is relatively weak.

3.6. Mechanism of the Enhancement of the Raman Bands of the Final Films on Gold. The Raman spectra of the final films deposited on a gold support correspond to the aniline oligomers constituting the first molecular layer adsorbed on the metallic surface at the beginning of the reaction. The Raman spectra of the final films obtained in the presence of succinic acid or in water on the gold substrate are very close but not identical with the Raman spectra of aniline oligomers precipitated on silicon windows in the first phase of the reaction. The peaks observed at 1589, 1541, 1480, 1412, 1363, 1270, 1240, and 1157 cm^{-1} in the spectrum of the starting films deposited on the silicon window are slightly shifted to 1594, 1568, 1514, 1476, 1420, 1373, 1250, and 1162 cm^{-1} in the spectra of the final films deposited on the gold support (Figure 10), and the total enhancement of their intensity is relatively low.

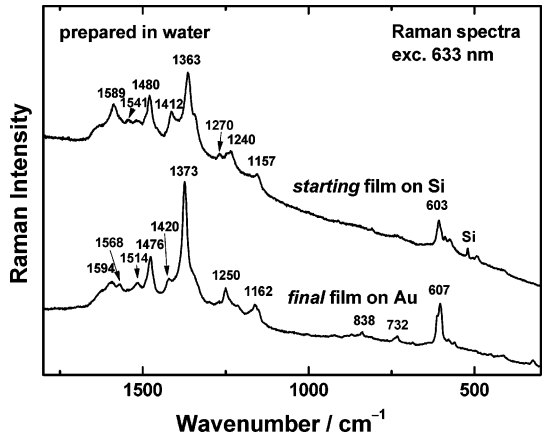

Figure 10. Raman spectrum of the starting film produced during the oxidation of aniline in water on silicon window separated from the reaction mixture after 8 min from the beginning of the reaction and the Raman spectrum of the final film deposited on gold.

Because the fact that the excitation of plasmons at smooth surfaces is not possible, we suppose that the increase in Raman scattering of adsorbed oligomers is caused by a resonance-like Raman effect. This so-called chemical (or molecular) mechanism of SERS lies in the increased Raman cross-section as a result of the surface interaction. The oligomers are expected to be chemisorbed at the metal SERS-active sites, which allows the formation of a charge-transfer complex between the molecule and an optically-excited conducting electron at the gold surface. This expands the effective molecular polarizability.[71] The interaction of the oligomers with the gold support restrains the complete deprotonation of the film with ammonium hydroxide, which is the reason for the observation of the small peak at 1373 cm^{-1} of the C∼N^+ ring-stretching vibrations of charged phenazine-like units in the *N*-phenyl-substituted phenazinium cation in the Raman spectra of adsorbed aniline oligomers in the deprotonated final films produced during in situ oxidation of aniline in the presence of succinic acid or water on gold (Figure 5b).[34,70]

It is known that resonance of the excitation laser line 633 nm with the electronic transition of phenazine segments occurs. Phenazine- or oxazine-containing dyes, having a set of bands at about 1637, 1375, and 606 cm^{-1}, include a positively charged nitrogen atom.[45] Ferreira et al. observed peaks at 610 and 1370 cm^{-1} in the Raman spectra (obtained with 633 nm excitation) of the aniline oligomers synthetized with APS at pH 3 on a gold support and assigned them to ring-deformation vibrations and to the C∼N^+ ring-stretching vibrations, which were observed also in safranine and are associated with the presence of phenazine-like segments.[60] The presence of out-of-plane bands in the SERS spectra of Meldola blue was assigned to the flat or slightly tilted orientation of benzenoid rings at the surface.[72]

3.7. Application and Importance of Aniline Oligomers. Several reports have been written on the

fundamental role of aniline oligomers in guiding the shape of polyaniline nanostructures.[73−79] The oligomeric micro/nanostructures are formed during aniline oxidation by self-assembly of the reaction intermediates.[33,48,80,81] This proceeds in the medium containing the as-produced intermediates and by-products of aniline oxidation. The byproducts of the reaction, such as sulfuric acid and ammonium sulfate (Figure 1), strongly influence the pH as well as ion strength of the medium and, consequently, the self-assembly of the intermediates.[73−76] The competition between oligomer adsorption and self-assembly leads to the creation of microspheres, self-assembled sheets, and nanotubes or to the film formation on the surface. For this reason, we can find the same products inside the microspheres[70] or on the surface of the gold support.[60] In the self-assembly of oligomers, different specific interactions work simultaneously: $\pi-\pi$ attractions, hydrophobic interactions, or hydrogen-bonding are the controlling factors.[76] On silicon, a so-called repulsive surface, the self-assembly that gives rise to various supramolecular structures is prevailing. On gold, a so-called attractive surface, the molecule−molecule interactions in solution are perturbed by stronger molecule−surface interactions.[82] This interaction leads to the observed SERS of the adsorbed oligomers on gold and to the different Raman spectra of the final films on silicon and final films on gold supports. On the basis of the present study, we conclude that the formation of PANI micro/nanostructures or films is related to the presence of positively charged phenazine-like chromophores in the first products of aniline oxidation with APS.

The surface resonance Raman spectroscopy of the submonolayer of oligomers observed in the presence of bulk polyaniline film makes this method advantageous in surface science, with many applications. Independent investigation of aniline oligomers reveals that they exhibit many interesting properties,[61,77] such as the ability to reduce silver cations to silver, the presence of base−salt transition, and the ability to be carbonized to nitrogen-containing carbons.

4. CONCLUSIONS

The Raman spectra of the as-produced final films on a gold support strongly differ from the spectra of the final films produced on silicon, which correspond to the spectra obtained previously by other groups from the oxidation of aniline in the presence of strong or weak acids or in water. They are resonantly enhanced in the cases of a weak acid solution and water. They are very close to the Raman spectra of the products of aniline oxidation in the presence of strong and weak acids or in water deposited as the starting films on silicon windows.

These observations can be explained by resonance Raman scattering originating from the interfacial deposition of aniline oligomers at the early stages of the reaction and their interaction with the gold surface. The sharp band at 1378 cm^{-1} observed in the Raman spectrum of the final film on gold and at 1363 cm^{-1} of the starting films on silicon corresponds to the C∼N^+ vibrations of charged phenazine-like units in the *N*-phenyl-substituted phenazinium cation, which is related to the adsorbed oligomers on the surface.

The association of the sharp peak at about 1373 cm^{-1} in the Raman spectra of the as-produced first products of aniline oxidation with APS (starting films) on silicon or of the as-produced final films on the gold support with the C∼N^+ vibrations in the *N*-phenyl-substituted phenazinium cation was confirmed by the calculated Raman spectra. This peak has not been observed in the calculated Raman spectra of the deprotonated samples.

The surface resonance Raman spectroscopy of the submonolayer of oligomers observed in the presence of bulk polyaniline film makes this method advantageous in surface science, with many applications in electrochemistry, catalysis, and biophysical, polymer, and analytical chemistry.

AUTHOR INFORMATION

Corresponding Author

*E-mail: trchova@imc.cas.cz.

Author Contributions

The manuscript was written through contributions of all authors. All authors have given approval to the final version of the manuscript.

Notes

The authors declare no competing financial interest.

ACKNOWLEDGMENTS

The support of the Czech Science Foundation (P205/12/0911 and 13-00270S) is gratefully acknowledged.

REFERENCES

(1) Soto-Oviedo, M. A.; Araújo, O. A.; Faez, R.; Rezende, M. C.; De Paoli, M.-A. *Synth. Met.* **2006**, *156*, 1249−1255.
(2) Deepshikha; Basu, T. *Anal. Lett.* **2011**, *44*, 1126−1171.
(3) Wan, D.; Yuan, S.; Li, G. L.; Neoh, K. G.; Kang, E. T. *ACS Appl. Mater. Interfaces* **2010**, *2*, 3083−3091.
(4) Karpakam, V.; Kamaraj, K.; Sathiyanarayanan, S.; Venkatachari, G.; Ramu, S. *Electrochim. Acta* **2011**, *56*, 2165−2173.
(5) Chen, F.; Liu, P. *ACS Appl. Mater. Interfaces* **2011**, *3*, 2694−2702.
(6) Deshpande, P. P.; Vathare, S. S.; Vagge, S. T.; Tomšík, E.; Stejskal, J. *Chem. Pap.* **2013**, *67*, 1072−1078.
(7) Sun, L. J.; Liu, X. X.; Lau, K. K. T.; Chen, L.; Gu, W. M. *Electrochim. Acta* **2008**, *53*, 3036−3042.
(8) Miao, Y. E.; Fan, W.; Chen, D.; Liu, T. *ACS Appl. Mater. Interfaces* **2013**, *5*, 4423−4428.
(9) Fan, W.; Zhang, Ch.; Tjiu, W. W.; Pramoda, K. P.; He, Ch.; Liu, T. *ACS Appl. Mater. Interfaces* **2013**, *5*, 3382−3391.
(10) Li, Z. F.; Zhang, H.; Liu, Q.; Sun, L.; Stanciu, L.; Xie, J. *ACS Appl. Mater. Interfaces* **2013**, *5*, 2685−2691.
(11) Zhao, D.; Guo, X.; Gao, Y.; Gao, F. *ACS Appl. Mater. Interfaces* **2012**, *4*, 5583−5589.
(12) Yeh, Y. R.; Hsiao, H. T.; Wu, C. G. *Synth. Met.* **2001**, *121*, 1651−1652.
(13) Bessière, A.; Duhamel, C.; Badot, J. C.; Lucas, V.; Certiat, M. C. *Electrochim. Acta* **2004**, *49*, 2051−2055.
(14) Tan, F. R.; Qu, S. C.; Wu, J.; Wang, Z. J.; Jin, L.; Bi, Y.; Cao, J.; Liu, K.; Zhang, J. M.; Wang, Z. G. *Sol. Energy Mater. Sol. Cells* **2011**, *95*, 440−445.
(15) Michel, M.; Bour, J.; Petersen, J.; Arnoult, C.; Ettingshausen, F.; Roth, C. *Fuel Cells* **2010**, *10*, 932−937.
(16) Wu, C. G.; Hsiao, H. T.; Yeh, Y. R. *J. Mater. Chem.* **2001**, *11*, 2287−2292.
(17) Wang, C. H.; Chen, C. C.; Hsu, H. C.; Du, H. Y.; Chen, C. P.; Hwang, J. Y.; Chen, L. C.; Shih, H. C.; Stejskal, J.; Chen, K. H. *J. Power Sources* **2009**, *190*, 279−284.
(18) Blinova, N. V.; Stejskal, J.; Frechet, J. M. J.; Svec, F. *J. Polym. Sci., Part A: Polym. Chem.* **2012**, *50*, 3077−3085.
(19) Halvorson, C.; Cao, Y.; Moses, D.; Heeger, A. J. *Synth. Met.* **1993**, *57*, 3941−3944.
(20) Srivastava, S.; Kumar, S.; Singh, V. N.; Singh, M.; Vijay, Y. K. *Int. J. Hydrogen Energy* **2011**, *36*, 6343−6355.
(21) Singh, J.; Bhondekar, A. P.; Singla, M. L. *ACS Appl. Mater. Interfaces* **2013**, *5*, 5346−5357.

(22) Kim, B. R.; Lee, H. K.; Park, S. H.; Kim, H. K. *Thin Solid Films* **2011**, *519*, 3492−3496.
(23) Tantawy, H. R.; Aston, D. E.; Smith, J. R.; Young, J. L. *ACS Appl. Mater. Interfaces* **2013**, *5*, 4648−4658.
(24) Stejskal, J. *Chem. Pap.* **2013**, *67*, 814−848.
(25) Xu, P.; Zhang, B.; Mack, N. H.; Doorn, S. K.; Han, X.; Wang, H. L. *J. Mater. Chem.* **2010**, *20*, 7222−7226.
(26) Yan, J.; Han, X.; He, J.; Kang, L.; Zhang, B.; Du, Y.; Zhao, H.; Dong, C.; Wang, H. L.; Xu, P. *ACS Appl. Mater. Interfaces* **2012**, *4*, 2752−2756.
(27) Li, S.; Xu, P.; Ren, Z.; Du, Y.; Han, X.; Mack, N. H.; Wang, H. L. *ACS Appl. Mater. Interfaces* **2013**, *5*, 49−54.
(28) Qian, K.; Liu, H. L; Yang, L. B.; Liu, J. H. *Nanoscale* **2012**, *4*, 6449−6454.
(29) He, J.; Han, X.; Yan, J.; Kang, L.; Zhang, B.; Du, Y.; Dong, C.; Wang, H. L.; Xu, P. *CrystEngComm* **2012**, *14*, 4952−4954.
(30) Mai, F. D.; Yu, C. C.; Liu, Y.C.; Yang, K. H.; Juang, M. Y. *J. Phys. Chem. C* **2011**, *115*, 13660−13666.
(31) Stejskal, J.; Sapurina, I. *Pure Appl. Chem.* **2005**, *77*, 815−826.
(32) Stejskal, J.; Sapurina, I.; Trchová, M.; Konyushenko, E. N. *Macromolecules* **2008**, *41*, 3530−3536.
(33) Trchová, M.; Šeděnková, I.; Konyushenko, E. N.; Stejskal, J.; Holler, P.; Ćirić-Marjanović, G. *J. Phys. Chem. B* **2006**, *110*, 9461−9468.
(34) Ćirić-Marjanović, G.; Trchová, M.; Stejskal, J. *J. Raman Spectrosc.* **2008**, *39*, 1375−1387.
(35) Saheb, A. M.; Seo, S. S. *Anal. Lett.* **2011**, *44*, 1206−1216.
(36) Trchová, M.; Morávková, Z.; Šeděnková, I.; Stejskal, J. *Chem. Pap.* **2012**, *66*, 415−445.
(37) Davidson, R. A.; Guo, T. *J. Phys. Chem. Lett.* **2012**, *3*, 3271−3275.
(38) Izumi, C. M. S.; Andrade, G. F. S.; Temperini, M. L. A. *J. Phys. Chem. B* **2008**, *112*, 16334−16340.
(39) Cochet, M.; Louarn, G.; Quillard, S.; Buisson, J. P.; Lefrant, S. *J. Raman Spectrosc.* **2000**, *31*, 1041−1049.
(40) Baibarac, B.; Mihut, L.; Louarn, G.; Mevellec, J. Y.; Wery, J.; Lefrant, S.; Baltog, I. *J. Raman Spectrosc.* **1999**, *30*, 1105−1113.
(41) Baibarac, M.; Mihut, L.; Louarn, G.; Lefrant, S.; Baltog, I. *J. Polym. Sci., Part B: Polym. Phys.* **2000**, *38*, 2599−2609.
(42) Šeděnková, I.; Trchová, M.; Stejskal, J. *Polym. Degrad. Stab.* **2008**, *93*, 2147−2157.
(43) Rozlívková, Z.; Trchová, M.; Šeděnková, I.; Špírková, M.; Stejskal, J. *Thin Solid Films* **2011**, *519*, 5933−5941.
(44) da Silva, J. E. P.; de Faria, D. L. A.; de Torresi, S. I. C.; Temperini, M. L. A. *Macromolecules* **2000**, *33*, 3077−3083.
(45) do Nascimento, G. M.; Temperini, M. L. A. *J. Raman Spectrosc.* **2008**, *39*, 772−778.
(46) do Nascimento, G. M.; da Silva, C. H. B.; Temperini, M. L. A. *Polym. Degrad. Stab.* **2008**, *93*, 291−297.
(47) Trchová M.; Morávková Z.; Bláha M.; Stejskal J. *Electrochim. Acta* [Online early access]. DOI: 10.1016/j.electacta.2013.10.133. Published Online: Nov 1, **2013**.
(48) Stejskal, J.; Sapurina, I.; Trchová, M. *Prog. Polym. Sci.* **2010**, *35*, 1420−1481.
(49) Frisch, M. J.; Trucks, G. W.; Schlegel, H. B.; Scuseria, G. E.; Robb, M. A.; Cheeseman, J. R.; Scalmani, G.; Barone, V.; Mennucci, B.; Petersson, G. A.; Nakatsuji, H.; Caricato, M.; Li, X.; Hratchian, H. P.; Izmaylov, A. F.; Bloino, J.; Zheng, G.; Sonnenberg, J. L.; Hada, M.; Ehara, M.; Toyota, K.; Fukuda, R.; Hasegawa, J.; Ishida, M.; Nakajima, T.; Honda, Y.; Kitao, O.; Nakai, H.; Vreven, T.; Montgomery, Jr., J. A.; Peralta, J. E.; Ogliaro, F.; Bearpark, M.; Heyd, J. J.; Brothers, E.; Kudin, K. N.; Staroverov, V. N.; Kobayashi, R.; Normand, J.; Raghavachari, K.; Rendell, A.; Burant, J. C.; Iyengar, S. S.; Tomasi, J.; Cossi, M.; Rega, N.; Millam, J. M.; Klene, M.; Knox, J. E.; Cross, J. B.; Bakken, V.; Adamo, C.; Jaramillo, J.; Gomperts, R.; Stratmann, R. E.; Yazyev, O.; Austin, A. J.; Cammi, R.; Pomelli, C.; Ochterski, J. W.; Martin, R. L.; Morokuma, K.; Zakrzewski, V. G.; Voth, G. A.; Salvador, P.; Dannenberg, J. J.; Dapprich, S.; Daniels, A. D.; Farkas, Ö.; Foresman, J. B.; Ortiz, J. V.; Cioslowski, J.; Fox, D. J. *Gaussian 09*, revision C.01; Gaussian, Inc.: Wallingford, CT, 2010.
(50) Merrick, J. P.; Moran, D.; Radom, L. *J. Phys. Chem. A* **2007**, *111*, 11683−11700.
(51) Trchová, M.; Šeděnková, I.; Stejskal, J. *Synth. Met.* **2005**, *154*, 1−4.
(52) Tomšík, E.; Morávková, Z.; Stejskal, J.; Trchová, M.; Zemek, J. *Synth. Met.* **2012**, *162*, 2401−2405.
(53) do Nascimento, G. M.; Silva, C. H. B.; Izumi, C. M. S.; Temperini, M. L. A. *Spectrochim. Acta, Part A* **2008**, *71*, 869−875.
(54) do Nascimento, G. M.; Kobata, P. Y. G.; Millen, R. P.; Temperini, M. L. A. *Synth. Met.* **2007**, *157*, 247−251.
(55) Colomban, Ph.; Gruger, A.; Novak, A.; Régis, A. *J. Mol. Struct.* **1994**, *317*, 261−271.
(56) Dmitrieva, E.; Harima, Y.; Dunsch, L. *J. Phys. Chem. B* **2009**, *113*, 16131−16141.
(57) Dmitrieva, E.; Dunsch, L. *J. Phys. Chem. B* **2011**, *115*, 6401−6411.
(58) Kellenberger, A.; Dmitrieva, E.; Dunsch, L. *Phys. Chem. Chem. Phys.* **2011**, *13*, 3411−3420.
(59) Surwade, S. P.; Dua, V.; Manohar, N.; Manohar, S. K.; Beck, E.; Ferraris, J. P. *Synth. Met.* **2009**, *159*, 445−455.
(60) Ferreira, D. C.; Pires, J. R.; Temperini, M. L. A. *J. Phys. Chem. B* **2011**, *115*, 1368−1375.
(61) Stejskal, J.; Trchová, M. *Polym. Int.* **2012**, *61*, 240−251.
(62) Marjanović, B.; Juranić, I.; Ćirić-Marjanović, G. *J. Phys. Chem. A* **2011**, *115*, 3536−3550.
(63) Ćirić-Marjanović, G. *Synth. Met.* **2013**, *177*, 1−47.
(64) Silva, C. H. B.; Ferreira, D. C.; Constantino, V. R. I.; Temperini, M. L. A. *J. Raman Spectrosc.* **2011**, *42*, 1653−1659.
(65) Silva, C. H. B.; Ferreira, D. C.; Rômulo, A. A.; Temperini, M. L. A. *Chem. Phys. Lett.* **2012**, *551*, 130−133.
(66) Niaura, G.; Mažeikienė, R.; Malinauskas, A. *Synth. Met.* **2004**, *145*, 105−112.
(67) Mažeikienė, R.; Statino, A.; Kuodis, Z.; Niaura, G.; Malinauskas, A. *Electrochem. Commun.* **2006**, *8*, 1082−1086.
(68) Ćirić-Marjanović, G.; Trchová, M.; Stejskal, J. *Collect. Czech. Chem. Commun.* **2006**, *71*, 1407−1426.
(69) Ćirić-Marjanović, G.; Trchová, M.; Stejskal, J. *Int. J. Quantum Chem.* **2008**, *108*, 318−333.
(70) Morávková, Z.; Trchová, M.; Tomšík, E.; Zhigunov, A.; Stejskal, J. *J. Phys. Chem. C* **2013**, *117*, 2289−2299.
(71) Otto, A. *J. Raman Spectrosc.* **2005**, *36*, 495−509.
(72) Mažeikienė, R.; Niaura, G.; Eicher-Lorka, O.; Malinauskas, A. *J. Colloid Interface Sci.* **2011**, *357*, 189−197.
(73) Li, Y.; He, W.; Feng, J.; Jing, X. *Colloid Polym. Sci.* **2012**, *290*, 817−828.
(74) Li, Y.; Zheng, J. L.; Feng, J.; Jing, X. L. *Chem. Pap.* **2013**, *67*, 876−890.
(75) Zhao, Y. C.; Tomšík, E.; Wang, J. X.; Morávková, Z.; Zhigunov, A.; Stejskal, J.; Trchová, M. *Chem.—Asian J.* **2013**, *8*, 129−137.
(76) Zhao, Y. C.; Stejskal, J.; Wang, J. X. *Nanoscale* **2013**, *5*, 2620−2626.
(77) Wang, Y.; Tran, H. D.; Kaner, R. B. *Macromol. Rapid Commun.* **2011**, *32*, 35−49.
(78) Leng, W.; Zhou, S.; Wu, L. *Macromol. Chem. Phys.* **2011**, *212*, 1900−1909.
(79) Leng, W.; Zhou, S.; You, B.; Wu, L. *J. Colloid Interface Sci.* **2012**, *374*, 331−338.
(80) Zujovic, Z. D.; Laslau, C.; Bowmaker, G. A.; Kilmartin, P. A.; Webber, A. L.; Brown, S. P.; Travas-Sejdic, J. *Macromolecules* **2010**, *43*, 662−670.
(81) Laslau, C.; Zujovic, Z.; Travas-Sejdic, J. *Prog. Polym. Sci.* **2010**, *35*, 1403−1419.
(82) Hoeben, F. J. M.; Jonkheijm, P.; Meijer, E. W.; Schenning, A. P. H. *Chem. Rev.* **2005**, *105*, 1491−1546.